



THE UNIVERSITY *of* EDINBURGH

Edinburgh Research Explorer

Intracellular potassium under osmotic stress determines the dielectrophoresis cross-over frequency of murine myeloma cells in the MHz range

Citation for published version:

Chung, C, Pethig, R, Smith, S & Waterfall, M 2018, 'Intracellular potassium under osmotic stress determines the dielectrophoresis cross-over frequency of murine myeloma cells in the MHz range', *Electrophoresis*.
<https://doi.org/10.1002/elps.201700433>

Digital Object Identifier (DOI):

[10.1002/elps.201700433](https://doi.org/10.1002/elps.201700433)

Link:

[Link to publication record in Edinburgh Research Explorer](#)

Document Version:

Peer reviewed version

Published In:

Electrophoresis

General rights

Copyright for the publications made accessible via the Edinburgh Research Explorer is retained by the author(s) and / or other copyright owners and it is a condition of accessing these publications that users recognise and abide by the legal requirements associated with these rights.

Take down policy

The University of Edinburgh has made every reasonable effort to ensure that Edinburgh Research Explorer content complies with UK legislation. If you believe that the public display of this file breaches copyright please contact openaccess@ed.ac.uk providing details, and we will remove access to the work immediately and investigate your claim.





Intracellular potassium under osmotic stress determines the dielectrophoresis cross-over frequency of murine myeloma cells in the MHz range.

| | |
|-------------------------------|--|
| Journal: | <i>ELECTROPHORESIS</i> |
| Manuscript ID | elps.201700433.R1 |
| Wiley - Manuscript type: | Research Paper |
| Date Submitted by the Author: | n/a |
| Complete List of Authors: | Chung, Colin; The University of Edinburgh, Institute for Integrated Micro & Nanosystems Pethig, Ronald ; The University of Edinburgh, School of Engineering Smith, Stewart; The University of Edinburgh, Institute for Bioengineering Waterfall, Martin; The University of Edinburgh, School of Biological Sciences |
| Keywords: | Dielectrophoresis, Intracellular potassium, High frequency DEP cross-over, Murine myeloma cells, Osmotic stress |
| | |

1
2
3 Research Paper
4
5
6

7 **Intracellular potassium under osmotic stress determines the dielectrophoresis**
8
9 **cross-over frequency of murine myeloma cells in the MHz range**
10

11 Colin Chung^{1*}, Ronald Pethig¹, Stewart Smith², Martin Waterfall³.
12
13

14
15 School of Engineering, ¹Institute for Integrated Micro & Nanosystems,
16

17 ²Institute for Bioengineering, University of Edinburgh, Edinburgh, UK;
18

19 *Present address: Cirrus Logic International (UK) Ltd., Quartermile, Edinburgh.
20

21 ³Institute of Immunology & Infection Research, School of Biological Sciences,
22
23 University of Edinburgh, Edinburgh, UK
24
25
26
27
28

29 **Keywords:**

30
31 Dielectrophoresis / Intracellular potassium / High frequency cross-over / Murine
32
33 myeloma cells / Osmotic stress /
34
35
36

37 **Communicating Author:** Professor Ronald Pethig
38

39 Postal address (for galley proofs):
40

41 Lleyn,
42

43 Telford Road,
44

45 Menai Bridge
46

47 Anglesey LL59 5DT,
48

49 UK
50

51 Ron.Pethig@ed.ac.uk
52
53
54
55
56
57
58
59
60

Abstract:

Dielectrophoresis (DEP) has been widely studied for its potential as a biomarker-free method of sorting and characterizing cells based upon their dielectric properties. Most studies have employed voltage signals from ~ 1 kHz to no higher than ~ 30 MHz. Within this range a transition from negative to positive DEP can be observed at the cross-over frequency f_{x01} . The value of f_{x01} is determined by the conductivity of the suspending medium, as well as the size and shape of the cell and the dielectric properties (capacitance, conductivity) of its plasma membrane. In this work DEP measurements were performed up to 400 MHz, where the transition from positive to negative DEP can be observed at a higher cross-over frequency f_{x02} . SP2/O murine myeloma cells were suspended in buffer media of different osmolarities and measurements taken of cell volume, f_{x01} and f_{x02} . Potassium-binding benzofuran isophthalate (PBFI), a potassium-sensitive fluorophore, and flow cytometry was employed to monitor relative changes in intracellular potassium concentration. In agreement with theory, it was found that f_{x02} is independent of the cell parameters that control f_{x01} and is predominantly determined by intracellular conductivity. In particular, the value of f_{x02} is highly correlated to that of the intracellular potassium concentration.

1 Introduction

Under appropriate experimental conditions both theory [1-3] and experiment (*e.g.*, [4-5]) show that dielectrophoresis (DEP) of viable mammalian cells exhibits three modes of behaviour with increasing frequency of the applied electric field. At the so-called ‘cross-over’ frequency f_{x01} a transition from negative to positive DEP occurs, whilst at the much higher frequency f_{x02} there is a transition back to negative DEP [6,7]). At f_{x01} and f_{x02} the DEP force is zero, corresponding to the effective dielectric properties of the cell exactly matching those of the volume of suspending medium displaced by the cell. Because the value of f_{x01} is sensitive to the shape of a cell, the dielectric properties of spherical, ellipsoidal and discoid cells can be evaluated if appropriate geometrical parameters are employed [8-10]. This paper describes investigations of the little explored characteristics of f_{x02} , and to place this into context it is useful to summarise the current situation regarding f_{x01} .

As reviewed elsewhere [10-14], theoretical and experimental evaluations of f_{x01} have been extensive and exploited in practical applications of DEP, such as the manipulation, separation, and isolation of target cells from mixtures in suspension. Taking into account typical values for the size and dielectric properties of mammalian cells, f_{x01} to a very good approximation is given by [15, 16]:

$$f_{x01} = \frac{\sqrt{2}}{2\pi RC_m} \sigma_s - \frac{\sqrt{2}}{8\pi C_m} G_m \quad (1)$$

In this equation R is the radius of a spherical cell, or the equivalent radius $(abc)^{1/3}$ of an ellipsoid with radii a , b , c , when suspended in a medium of conductivity σ_s . C_m and G_m are the capacitance and conductance of the cell membrane (per unit area).

1
2
3 Equation (1) is derived by applying the low-frequency DC approximations proposed
4 by Schwan [17] for the effective conductivity ($\sigma_{eff} = RG_m$) and permittivity
5 ($\epsilon_{eff} = RC_m$) of a cell. Values for C_m can be obtained [16] from the slope of the
6
7
8 plot of $f_{xo1} \cdot R$ against σ_s , but accurate values for G_m derived from the intercept of such
9
10
11 plots are only possible for restricted values of the frequency and medium conductivity
12
13 [18]. The 2nd term on the right-hand side of Equation (1) is typically ~100-times
14
15 smaller than the 1st term and is often neglected [11,19]. Determination of C_m can then
16
17
18 be made from measurements of f_{xo1} and R at a known value for σ_s , but with the risk
19
20
21 that the onset of passive ionic conductance due to degradation of the membrane's
22
23
24 integrity will lead to significant underestimation of C_m .
25
26
27

28
29 Gascoyne *et al* [19] have summarised how C_m varies substantially between different
30
31 cell types; cells in different states of differentiation; in different stages of the cell
32
33 cycle; and following exposure of cells to apoptosis-inducing agents and toxicants. It
34
35 was concluded that variations in C_m are related to membrane surface features such as
36
37 ruffles, folds, and microvilli [20, 21], with the possibility that changes of membrane
38
39 structure and chemistry should also be taken into account [22]. Whereas cell size
40
41 does contribute significantly to dielectric differences between different cancer cell
42
43 types, the value for C_m can also vary significantly among cells of the same size.
44
45
46 Furthermore, under the same conditions, cancer cells exhibit consistently lower f_{xo1}
47
48 values than peripheral blood cells [19]. These factors are of great significance
49
50 regarding the development of DEP as a surface-marker independent and competitive
51
52 technique for isolating circulating tumour cells from peripheral blood [23, 24].
53
54
55
56
57
58
59
60

Detailed experimental measurements of f_{x02} for mammalian cells are, to our knowledge, restricted to an earlier report of our own for murine myeloma cells [25]. Values for f_{x02} were observed in the region of 200 MHz, in agreement with theory based on known cell dielectric parameters. An unexpected finding was that f_{x02} decreased steadily with time, in a temperature-activated (Arrhenius) manner. At 37°C, for example, f_{x02} fell from ~200 MHz to ~80MHz after 2 hrs of suspension in the DEP medium. In this work we have extended our earlier study to clarify the factors influencing the value of f_{x02} . We conclude that f_{x02} is sensitive to the intracellular conductivity, a factor correlated to the osmotically induced alteration of internal potassium ion concentration. To achieve this result, the drift in f_{x02} value was reduced to less than 10 MHz by performing the DEP measurements at 21°C and within 30 minutes of the cells being suspended in the DEP medium.

2 THEORY

A cells' DEP frequency response is defined by the Clausius-Mossotti factor [1-3]:

$$\frac{\varepsilon_c^* - \varepsilon_s^*}{\varepsilon_c^* + 2\varepsilon_s^*} \quad (2)$$

The parameters ε_c^* and ε_s^* represent the complex permittivities of the cell and its suspending medium, which consist of electrically lossy dielectrics defined by:

$$\varepsilon^* = \varepsilon_0 \varepsilon - \frac{j\sigma}{\omega} \quad (3)$$

where ε is the relative permittivity, ε_0 the permittivity of free space, σ the conductivity, ω the electric field angular frequency and j the imaginary vector, $\sqrt{-1}$. Equation (3) may be substituted directly into Equation (2) for the suspending medium,

1
2
3 which is effectively homogenous. A corresponding expression for the cell depends
4 upon its heterogeneous structure and the frequencies under consideration. At
5 sufficiently high frequencies, typically beyond 10 MHz and for a medium of 50 mS/m
6 conductivity [10], the resistance of the plasma membrane is effectively short circuited
7 by its capacitance, allowing the electric field to penetrate the cell interior.
8 Understanding the behaviour of cells at these frequencies therefore requires a model
9 incorporating their intracellular structure and dielectric properties. In the approach
10 taken by Asami *et al* [26], a multi-shelled model built from concentric spheres was
11 fitted to impedance measurements of mouse lymphocytes between 100 Hz and 250
12 MHz. Their model incorporated both the radii and complex permittivities of the cell
13 membrane, cytoplasm, nuclear envelope and nucleoplasm. By substituting an
14 effective expression for the complex permittivity of this structure into Equation (2) a
15 nucleated cell's DEP frequency spectrum can be predicted [26]. An example for
16 mouse lymphocytes is shown in Figure 1, modelled for three medium conductivities
17 using the dielectric properties of the cell compartments derived by Asami *et al* [26].
18 In agreement with Equation (1) the value for f_{x01} varies with changes in the medium
19 conductivity σ_s , whereas f_{x02} remains constant.

20
21
22
23
24
25
26
27
28
29
30
31
32
33
34
35
36
37
38
39
40
41
42 An analytical expression for f_{x02} was first derived by Gimsa *et al* [6] and later
43 simplified by Broche *et al* [27] to the following analytical expression:
44

$$45 \quad f_{x02} = \frac{\sigma_i}{2\pi\epsilon_0} \sqrt{\frac{1}{2\epsilon_s^2 - \epsilon_i\epsilon_s - \epsilon_i^2}} \quad (4)$$

46
47
48
49
50
51 where σ_i is the effective conductivity of the cell interior, and ϵ_0 , ϵ_s , ϵ_i are the
52 permittivity values of free space, the suspending medium and the cell interior,
53 respectively. This formula may also be derived directly by assuming that the imposed
54
55
56
57
58
59
60

1
2
3 electric field frequency is significantly beyond that associated with Maxwell-Wagner
4 interfacial polarisation of the plasma membrane. In this case the cell appears
5 essentially as the cytoplasm with its internal contents [3]. This can be modelled as a
6 multi-shelled dielectric sphere using the dielectric parameters for the cytoplasm and
7 nucleus derived by Asami *et al* [26]. Equation (4) is then derived by assuming that
8 the conductivity of the suspending medium is significantly below the intracellular
9 value, a condition which can be satisfied experimentally. The proportionality of f_{x02}
10 with respect to intracellular conductivity, as indicated by Equation (4), breaks down in
11 the limits of low intracellular and high medium conductivities [28]. For example, a
12 deviation of 9% in the predicted value for f_{x02} occurs when intracellular conductivity
13 reduces by 50% in a 300 mS/m medium. However, with the suspending medium
14 conductivity of 50 mS/m chosen for our experiments, the deviation from a direct 1:1
15 proportionality of f_{x02} with the intracellular conductivity was no more than 1%.
16 Finally, Equation (4) indicates that f_{x02} , in sharp contrast with f_{x01} , should be
17 independent of cell radius R , membrane capacitance C_m , membrane conductance G_m ,
18 and the conductivity σ_s of the cell suspending medium.
19
20
21
22
23
24
25
26
27
28
29
30
31
32
33
34
35
36
37
38
39
40

41 Intracellular dielectric properties are difficult to measure in practice and typically
42 require the fitting of multi-shelled dielectric models to impedance, electrorotation or
43 DEP measurements across a range of frequencies. In this work we restricted
44 ourselves to studying the changes in f_{x02} as a function of intracellular potassium ion
45 concentration $[K^+]_i$ - the most abundant intracellular ion [29]. Hypo-osmotic stress
46 was used as a means of diluting the intracellular compartment, the reducing $[K^+]_i$, and
47 with it the conductivity σ_i and, from Equation (4), the frequency f_{x02} . Hypo-osmotic
48
49
50
51
52
53
54
55
56
57
58
59
60

1
2
3 stress was first explored by Kregenow [30] to induce the efflux of potassium from
4 duck erythrocytes and later by Chimote [31] with human lens epithelial cells. We
5 applied a similar stress by suspending cells in a medium nearly devoid of potassium,
6 sodium or chloride ions and used mannitol to adjust osmolarity. Changes to $[K^+]_i$
7 were measured by ratiometric flow cytometry using a potassium sensitive fluorescent
8 dye [32-34]. By measuring the volume of cells for a range of medium osmolalities we
9 aimed to determine if a simple dilution model could account for the relative
10 differences induced in both $[K^+]_i$ and f_{xO_2} , and whether these quantities are indeed
11 proportional to each other as we expect from Equation (4). In addition, measurements
12 of f_{xO_1} were made to provide information regarding the morphology and capacitance
13 of the plasma membrane, in line with existing studies [15, 16, 19-22].
14
15
16
17
18
19
20
21
22
23
24
25
26
27
28
29

30 **3 MATERIALS AND METHODS**

31 All reagents were obtained from Life Technologies Corp. unless otherwise specified.
32
33

34 **3.1 Cell Culture**

35 The murine myeloma cell line SP2/O-AG14 was obtained from the American Type
36 Culture Collection (Catalogue No. CRL1581). Cells were grown under standard
37 tissue culture conditions as a suspension in RPMI-1640 supplemented with 10% Fetal
38 Bovine Serum, 100 units/ μ g/ml penicillin-streptomycin (*i.e.*, 1:100 dilution of
39 supplier's stock) and incubated at 37°C in a 5% humidified CO₂ atmosphere. The
40 culture was maintained at a concentration typically between 0.25 and 1×10^6 cells/ml
41 with regular feeding at 2 day intervals. In preparation for the experiments, 15 ml of
42 SP2/O-AG14 cells were suspended at a density of 0.5×10^6 cells/ml and incubated
43 overnight for 24 hours.
44
45
46
47
48
49
50
51
52
53
54
55
56
57
58
59
60

3.2 Potassium Sensitive Dye

The measurement of $[K^+]_i$ using the potassium-sensitive dye benzofuran isophthalate (PBFI) has been demonstrated with a variety of cell types [32-34]. The acetoxymethyl (AM) ester form of PBFI was dissolved in dimethyl sulfoxide (DMSO) at a stock concentration of 10 μ M with 10 μ l added to the culture media. To facilitate loading, 10 μ l of Pluronic F-127 (20% w/v) was added and the cells incubated for 100 minutes. Extracellular PBFI was then removed by washing cells in fresh culture medium followed by an additional 60 minute incubation period. These loaded cells were suspended into phosphate buffered saline (PBS) and split for concurrent DEP and flow cytometry measurements. The cells were subsequently split and washed twice in 10 ml of DEP medium alongside a PBS control, with centrifugation between washes performed at 300g for 5 minutes.

3.3 DEP Cell-Suspending Media

Culture media contain a variety of components important for the long term maintenance and growth of cells. Typical formulations result in electrical conductivities of media exceeding 1 S/m. However, DEP measurements often require that the cells are suspended in a medium of conductivity less than 100 mS/m. This requirement demands the near complete removal of sodium and potassium chloride which constitute the main source of mobile, conducting ions. Our iso-osmotic (290 mOsm) formulation contained (in mM): 0.4 Ca^{2+} , 0.4 Mg^{2+} , 0.8 NO_3^- , 0.4 SO_4^{2-} , 11 glucose, 10 HEPES and 267 mannitol. HEPES acted as a pH buffer in place of the standard sodium bicarbonate system used with CO_2 , and the pH was adjusted to 7.4 using NaOH. Hypo-osmotic solutions were prepared at 140, 190, 215, and 240 mOsm by the removal of mannitol, with the resulting osmolarity measured using an

1
2
3 osmometer (Advanced Model 3300) and the conductivity determined as 42 mS/m
4
5 using an Oakton CON-510 meter.
6
7
8

9 **3.4 Determination of Intracellular K⁺ and Membrane Integrity**

10
11 A ratiometric measurement approach was used to determine relative internal
12
13 potassium concentration, where the ratio of photoemissions at a characteristic
14
15 wavelength is determined based on two distinct excitation wavelengths. This
16
17 approach eliminates the impact of variations from both dye uptake and leakage. PBFI
18
19 is relatively insensitive to changes in intracellular pH and intracellular sodium
20
21 concentrations below 75 mM, exhibiting a fluorescent ratio with a near linear
22
23 relationship to [K⁺]_i up to physiological levels [34]. Ratiometric measurements were
24
25 performed on washed cells by flow cytometry (BD Biosciences LSR II). Excitation
26
27 wavelengths of 355 and 405 nm were chosen which are close to the known excitation
28
29 maxima and isobestic point of PBFI [32, 33]. Emissions were measured at ~500 nm
30
31 and their ratio arising from excitations at both 355 and 405 nm were calculated.
32
33 These ratios were normalised to that obtained for control samples suspended in PBS
34
35 (~300 mOsm) and expressed as a percentage to provide a relative measurement of
36
37 intracellular potassium concentration.
38
39
40
41
42
43

44 Cytometric analysis using the membrane impermeant fluorescent dye propidium
45
46 iodide (PI) was employed to evaluate the proportion of apparently intact cells with
47
48 damaged cytoplasmic membranes [35] in samples used for DEP analysis. As
49
50 described in detail elsewhere [28] this technique provided information regarding the
51
52 physical stability of cells suspended in DEP media of different osmolarity values.
53
54
55
56
57
58
59
60

3.5 DEP Cross-over (f_{x01} , f_{x02}) and Cell Diameter Measurements

The device used for DEP characterisation is described fully elsewhere [25, 28]. In brief, an array of sixteen 100 nm thick, 20 μm wide, platinum interdigitated electrodes spaced 40 μm apart were vacuum deposited onto a glass substrate. The final design, with a total effective capacitance of ~ 5 pF, was based on investigations to explore the impact of array size, electrode separation and solution conductivity on an applied electric signal. A circuit model based on a distributed RC network was evaluated and found to provide close agreement with practical impedance measurements. This was used to predict the voltage and phase along the electrode elements. A surface-mounted 50 Ω resistor was connected in parallel with the electrode array, which was then soldered to a BNC connector to form a low pass filter. This arrangement provided a flat amplitude response below ~ 500 MHz, to ensure a constant field strength over the frequency range of interest, and was mounted into an inverted microscope (Meiji TC5100) equipped with a digital camera (Lumenera Infinity 2-3) for image capture.

Washed cells were suspended at a concentration of 1×10^7 cells/ml with 6.5 μl samples deposited onto the electrodes for analysis. A glass coverslip and gasket formed a chamber preventing any evaporation or disturbance of the sample. At the lower frequencies of f_{x01} an Agilent 3324A signal generator supplied a 5V pk-pk sinusoid from 25 to 300 kHz. The frequency was increased in steps of 25 kHz lasting 5 seconds, which at the lower frequencies caused cells to levitate under negative DEP before attraction to the electrode edges by positive DEP above f_{x01} . High frequency measurements of f_{x02} used an Agilent ESD-4000A signal generator and a Mini-Circuits ZHL-1A amplifier generating a 4V pk-pk sinusoid. In a symmetrical manner

1
2
3 to f_{x01} the frequency was swept downwards from 400 to 25 MHz in 5 seconds, 25
4
5 MHz steps, causing cells to initially levitate at high frequencies before being attracted
6
7 to the electrode edges at frequencies lower than f_{x02} . LabVIEW software controlled
8
9 the camera and signal generators with images captured at each frequency step. By
10
11 counting the cells that had been attracted, and then attached, by positive DEP to the
12
13 edge of electrodes in these images the number within each band for f_{x01} and f_{x02} was
14
15 determined. Cell diameter measurements were made by capturing images using a 40×
16
17 objective. ImageJ software [36] was used to measure a sample of at least one hundred
18
19 cells per datum using the various suspending media.
20
21
22
23
24

25
26 In previous work [25] we described how the value of f_{x02} for cells suspended in DEP
27
28 medium gradually decreased over time. The initial decrease of f_{x02} , at 19 MHz/hr at
29
30 21 °C for the first two hours, limited the time that the cells could be suspended. In
31
32 addition, the magnitude of the positive DEP force decreased steadily with time,
33
34 leading to difficulties in clear observation of the attraction of cells to electrodes. The
35
36 impact of this phenomenon was minimized by holding the PBF1-loaded cells in PBS
37
38 prior to washing them into their respective DEP media, with the subsequent
39
40 measurements performed within 30 minutes.
41
42
43
44

46 **4 RESULTS AND DISCUSSION**

47
48 Examples of forward (FSC) and side-scatter (SSC) plots are shown in Figure 2 for
49
50 cells suspended in culture medium and the various DEP media. The trend observed of
51
52 a reduction in FSC and an increase in SSC with increasing osmolarity is consistent
53
54 with a reduction of cell size due to osmotic pressure, together with a corresponding
55
56
57
58
59
60

1
2
3 concentration increase of intracellular content. Also shown in this Figure is the
4 percentage of intact cells in each sample, as determined by changes in the overall FSC
5 and SSC heights compared to those obtained at nominal time zero for cells suspended
6 in culture medium. In Figure 3 the FSC height versus PI fluorescence signal plots
7 show the effect of increasing osmotic stress. The gated regions highlight intact cells
8 with viable membranes, which when suspended in the original culture medium
9 comprised 63.1% of the cell population. The corresponding intact and viable
10 populations in the 270, 310 and 350 mOsm DEP media were 48.7%, 36.9% and
11 31.4%, respectively. As the osmolarity was reduced the median forward scatter
12 increased towards that of the culture medium. The proportion of whole cells, relative
13 to cell fragments, also increased. These distributions remained relatively constant up
14 to four hours following initial cell suspension. These measurements and observations,
15 described in more detail elsewhere [28], are consistent with the findings of Copp *et al*
16 [37] that hyperosmotic stress induces apoptosis in mammalian cells, through
17 inhibition of growth factor receptor signalling, induction of caspase-3 activation and
18 reversible fragmentation of mitochondrial structure. Only those cells that appeared to
19 be viable from their microscopic appearance (*e.g.*, typical size and no blebbing) were
20 studied for their DEP response.
21
22
23
24
25
26
27
28
29
30
31
32
33
34
35
36
37
38
39
40
41
42
43

44 As shown in the inset of Figure 4, the volume of cells loaded with PBF1 consistently
45 decreased as the medium osmolarity was increased. Cells suspended in 215 mOsm
46 DEP medium were found to have the same diameter, with similar relative forward and
47 side scatter, as cells suspended in PBS of osmolarity ~300 mOsm. This was taken to
48 indicate that for our mannitol-adjusted DEP media, the effective isotonic osmolarity
49 was 215 mOsm. Higher osmolalities resulted in cell shrinkage with ~30% decrease in
50
51
52
53
54
55
56
57
58
59
60

1
2
3 volume at 290 mOsm (corresponding to a decrease from the isotonic value of 897 ± 72
4
5 to $630\pm 51 \mu\text{m}^3$). This behaviour is similar to observations made by Rouzaire-Dubois
6
7 *et al* [38] for murine glioma cells suspended into a medium in which half of the
8
9 sodium chloride was substituted with sucrose. An observed 15% decrease in cell
10
11 volume, which occurred within minutes, was attributed to the efflux of Na^+ and Cl^-
12
13 due to their reduced extracellular concentrations. A study on human epithelial cells
14
15 by Hamann *et al* [39] implicated the $\text{Na}^+ - \text{K}^+ - 2\text{Cl}^-$ cotransporter NKCC1 in facilitating
16
17 this apparent isosmotic cell shrinkage under similar conditions. Our results suggest
18
19 that by applying hypo-osmotic stress the original cell volume can be maintained at the
20
21 effective isotonic osmolarity or increased further.
22
23

24
25
26
27 By plotting cell volume as a function of the inverse osmolarity, with both normalised
28
29 to the isotonic osmolarity of 215 mOsm, a linear relationship of the Boyle-van't Hoff
30
31 (BVH) form was found, as shown in Figure 4. The idealised BVH formula [40] is
32
33 given by:
34

$$\frac{V_{BVH}}{V_{iso}} = (1 - v_b) \frac{M_{iso}}{M} + v_b \quad (5)$$

35
36
37
38 where the modelled cell volume, V_{BVH} , and osmolarity, M , are normalised to the
39
40 measured isotonic values of V_{iso} and M_{iso} . The osmotically inactive fraction of the cell
41
42 volume v_b is represented by the intercept of this linear formula, which as shown in
43
44 Figure 4 is close to zero.
45
46
47
48
49

50
51 As shown in Figure 5 the mean value of f_{x01} decreased steadily with increasing
52
53 osmolarity of the medium. After an initial increase in value with increasing
54
55 osmolarity, f_{x02} remained fairly constant over the hypertonic range of our experiments.
56
57
58
59
60

This is the range in which cell shrinkage was observed. As f_{xO2} is proportional to intracellular conductivity it should also depend on the concentration of mobile ions. The observed behaviour of f_{xO2} is therefore consistent with a net loss of ions from the intracellular compartment. By contrast, hypotonic stress resulted in f_{xO2} decreasing by 35%, from its isotonic value of 166 ± 6 MHz to 108 ± 4 MHz at 140 mOsm. Assuming the concentration of mobile intracellular ions remains constant, the BVH model for cell volume can be used to scale the isotonic value of $f_{xO2(iso)}$. This dilution factor, the isotonic volume V_{iso} divided by the modelled volume V_{BVH} , yields the following behaviour for f_{xO2} :

$$f_{xO2(BVH)} = f_{xO2(iso)} \times \frac{V_{iso}}{V_{BVH}} \quad (6)$$

where $f_{xO2(BVH)}$ is the predicted value of f_{xO2} based upon the fitted BVH model. In Figure 5 this is shown as the dashed line and fits the hypotonic data with an R^2 value of 0.929. At 140 mOsm a 36% volume increase corresponds to a 35% decrease in f_{xO2} . Under hypertonic conditions the model breaks down, overestimating f_{xO2} and suggests that if f_{xO2} is proportional to the intracellular concentration of mobile ions an efflux must be occurring. Based on this we can predict the proportion n of ions lost due to hypertonic stress as:

$$n = 1 - \frac{f_{xO2(hyper)} \times V_{hyper}}{f_{xO2(iso)} \times V_{iso}} \quad (7)$$

where $f_{xO2(hyper)}$ and V_{hyper} are the hypertonic values for f_{xO2} and cell volume, respectively. Intracellular ion losses at 240 and 290 mOsm are estimated to be 18% and 29%, respectively. In the hypotonic region the value of n from Equation (7) remains close to zero.

1
2
3 DEP and ratiometric flow cytometry measurements were performed at the same time,
4 in parallel, using the same cell suspension medium. The fluorescence ratio of the
5 cells was calculated from their mean signal area intensity, and is plotted in Figure 6 as
6 a percentage relative to that of a PBS suspended control. Between 140 mOsm and the
7 isotonic value of 215 mOsm this ratio increased significantly, from $71 \pm 4\%$ to $94 \pm 5\%$.
8
9 Beyond this, the ratio increased only marginally to $99 \pm 6\%$ at 290 mOsm, which is a
10 small change by comparison to the concomitant 30% decrease in cell volume. A
11 physiological value for $[K^+]_i$ of 135 mM for our isotonic datum in DEP medium
12 would imply an increase to 176 mM at 290 mOsm, assuming no efflux of ions. The
13 fluorescent ratio is, however, known to behave in a non-linear manner at this
14 concentration and to approach a maximum value, which could account for such a
15 marginal increase in fluorescence [29]. By contrast, our observations of f_{xO2} strongly
16 suggest that an efflux of intracellular ions is occurring. As there is no clear consensus
17 between these two methods on the issue of hypertonic ion efflux, further study is
18 necessary. Dezaki *et al* [41] have observed that HeLa cells placed under hypertonic
19 stress observe an increase in $[K^+]_i$ and $[Cl^-]_i$ that is less than expected from the
20 associated decrease in volume, suggesting that a net efflux of both ions under such
21 conditions could indeed be occurring. As shown in Figure 7, a plot of f_{xO2} against the
22 relative fluorescence ratio reveals a strong correlation between these two parameters.
23
24 A straight line fit of the data gives an R^2 value of 0.967, which implies that f_{xO2} can
25 provide an effective means of characterising cells based on their intracellular
26 potassium concentration, particularly for those cells under isotonic or hypotonic
27 conditions.
28
29
30
31
32
33
34
35
36
37
38
39
40
41
42
43
44
45
46
47
48
49
50
51
52
53
54
55
56
57
58
59
60

1
2
3 The variation of membrane capacitance C_{mem} with osmolarity is shown in Figure 8,
4 and is consistent with previous studies [20]. The topographical changes involved can
5 be expressed as a morphological factor ϕ , given as the ratio of C_{mem} over a theoretical
6 value of 6 mF/m^2 for a typical smooth membrane [20]. At 140 mOsm, $\phi = 1.01$,
7 suggesting that our cells are extremely smooth and approaching the point of cytolysis.
8 The isotonic point corresponds to $\phi = 1.66$, increasing to $\phi = 2.41$ at 290 mOsm.
9 Broadly speaking, murine myeloma cells appear to behave as expected in terms of
10 hypo-osmotic stress, f_{x01} and cell volume.
11
12
13
14
15
16
17
18
19
20
21
22

23 5. Conclusions

24 This work has confirmed our earlier study [25] that measurement of the high-
25 frequency DEP cross-over frequency f_{x02} for mammalian cells is practicable. An
26 important conclusion is that f_{x02} is highly correlated to the intracellular conductivity,
27 and in particular to its potassium concentration.
28
29
30
31
32
33
34
35

36 Measurements of cell volume, f_{x01} , f_{x02} , and intracellular potassium were made under
37 varying degrees of osmotic stress. The cells closely obeyed the Boyle-van't Hoff
38 ideal osmometer model. From measurements of both f_{x01} and cell volume, the plasma
39 capacitance was found to trend in a linear manner with osmolarity, approaching the
40 expected value in the hypotonic extreme for a smooth lipid bilayer [20]. Over the
41 observed hypertonic range f_{x02} was found to be constant, indicating that an efflux of
42 intracellular ions occurred, proportionate to the volume of water lost. Under
43 increasing hypotonic stress the value of f_{x02} decreased in a linear manner, consistent
44 with a dilution of the intracellular ionic concentration resulting from the measured
45
46
47
48
49
50
51
52
53
54
55
56
57
58
59
60

1
2
3 increase in cell volume. Measurements using the potassium sensitive dye PBFI
4
5 revealed that under increasing hypotonic stress the concentration of potassium also
6
7 decreased in a linear manner, a relationship that strongly correlated to that of f_{x02} .
8
9

10
11
12 Introduction of f_{x02} as an investigative parameter can address new questions regarding
13
14 the internal physico-chemical nature of cells, with the potential to further expand the
15
16 analytical power of DEP. The critical role of potassium in many cell processes
17
18 including volume regulation, growth and apoptosis, emphasise its importance as a
19
20 biomarker. Our measurements of f_{x02} suggest that DEP can be used to discriminate
21
22 and sort cells based upon this. Although these initial studies reveal significant
23
24 potential for exploitation, the extent to which intracellular ions, cell cycle and
25
26 organelle structure affect f_{x02} remain areas that merit further research.
27
28
29

30
31 *We thank Drs Steve Pells, Vlastimil Srsen and David Wright for their practical*
32
33 *assistance and helpful discussions. This work was supported by a Wolfson*
34
35 *Microelectronics Scholarship awarded to C.C., and funding to RP from the*
36
37 *Edinburgh Research Partnership in Engineering and Mathematics (ERPem).*
38
39
40

41
42 *The authors declare no conflict of interest*
43
44

45 **6. References**

- 46
47 [1] Jones, T. B., *Electromechanics of Particles*, Cambridge University Press, New
48
49 York 1995.
50
51 [2] Morgan, H., Green, N. G., *AC Electrokinetics: Colloids and Nanoparticles*,
52
53 Research Studies Press, Baldock 2003.
54
55
56
57
58
59
60

- 1
2
3 [3] Pethig, R., *Dielectrophoresis: Theory, Methodology and Biological Applications*,
4 John Wiley & Sons, Chichester 2017.
5
6
7 [4] Adams, T. N. G., Turner, P. A., Janorkar, A. V., Zhao, F., Minerick, A. R.,
8 *Biomicrofluidics* 2014, 8, 054109.
9
10
11 [5] Faraghat, S. A., Hoettges, K. F., Steinbach, M. K., van der Veen, D. R.,
12 Brackenbury, W. J., Henslee, E. A., Labeed F. H., Hughes, M. P., *Proc. Natl. Acad.*
13 *Sci. USA* 2017, 114, 4591-4596.
14
15
16 [6] Gimsa, J., Marszalek, P., Loewe, U., Tsong, T. Y., *Biophys. J.* 1991, 60, 749-760.
17
18
19 [7] Wang, X-B., Pethig, R., Jones, T. B., *J. Phys. D: Appl. Phys.* 1992, 25, 905-912.
20
21
22 [8] Green, N. G., Jones, T. B., *J. Phys. D: Appl. Phys.* 2007, 40, 78-85.
23
24
25 [9] Sebastián, J. L., Muñoz, S., Sancho, M., Álvarez, G., Miranda, J. M., *Phys. Med.*
26 *Biol.* 2007, 52, 6831-6847.
27
28
29 [10] Lei U., Lo, Y. J., *IET Nanobiotechnology* 2011, 5, 86-106.
30
31 [11] Pethig, R., *Biomicrofluidics* 2010, 4, 02281.
32
33 [12] Cetin, B., Li, D., *Electrophoresis* 2011, 32, 2410-2427.
34
35 [13] Gagnon, Z. R., *Electrophoresis* 2011, 32, 2466-2487.
36
37 [14] R. Martinez-Duarte, R., *Electrophoresis* 2012, 33, 3110-3132.
38
39 [15] Huang, Y., Wang, X-B., Becker, F. F., Gascoyne, P. R. C., *Biochim. Biophys.*
40 *Acta*, 1996, 1282, 76-84.
41
42
43 [16] Pethig, R., Jakubek, L. M., Sanger, R. H., Heart, E., Corson, E. D., Smith, P. J. S.,
44 *IEE Proc. Nanobiotechnol.* 2005, 152, 189-193.
45
46
47 [17] Schwan, H. P., *Adv. Biol. Med. Phys.* 1957, 5, 147-209.
48
49
50 [18] Lei, U., Sun, P-H., Pethig, R., *Biomicrofluidics* 2011, 5, 044109.
51
52
53 [19] Gascoyne, P. R. C., Shim, S., Noshari, J., Becker, F. F., Stenke-Hale, K.,
54 *Electrophoresis* 2013, 34, 1042-1050.
55
56
57
58
59
60

- 1
2
3 [20] Wang, X-B., Huang, Y., Gascoyne, P. R. C., Becker, F. F., Hölzel, R., Pethig, R.,
4
5 *Biochim. Biophys. Acta* 1994, 1193, 330-344.
6
7 [21] Huang, Y., Wang, X-B., Gascoyne, P. R. C., Becker, F. F., *Biochim. Biophys.*
8
9 *Acta* 1999, 1417, 51-62.
10
11 [22] Muratore, M., Srsen, V., Waterfall, M., Downes, A., Pethig, R., *Biomicrofluidics*
12
13 2012, 6, 034113.
14
15 [23] Gupta, V., Jafferji, I., Garza, M., Melnikova, V., Hasegawa, D., Pethig, R., Davis,
16
17 D., *Biomicrofluidics* 2012, 6, 024133.
18
19 [24] Shim, S., Stemke-Hale, K., Tsimberidou, A. M., Noshari, J., Anderson, T. E.,
20
21 Gascoyne, P. R. C., *Biomicrofluidics* 2013, 7, 011808.
22
23 [25] Chung, C., Waterfall, M., Pells, S., Menachery, A., Smith, S., Pethig, R., *J.*
24
25 *Electr. Bioimp.* 2011, 2, 64-71.
26
27 [26] Asami, K., Takahashi, Y., Takashima, S., *Biochim. Biophys. Acta* 1989, 1010,
28
29 49-66.
30
31 [27] Broche, L. M., Labeed, F. H., Hughes, M. P., *Phys. Med. Biol.* 2005, 50, 2267-
32
33 2274.
34
35 [28] Chung, C., *Dielectrophoretic investigations of internal cell properties*, Ph.D
36
37 thesis, School of Engineering, The University of Edinburgh, 2015.
38
39 <http://hdl.handle.net/1842/10044>
40
41
42 [29] Yu, S. P., Canzoniero, L. M. T., Choi, D. W., *Curr. Opin. Cell Biol.* 2001, 13,
43
44 405-411.
45
46 [30] Kregenow, F. M., *J. Gen. Physiol.* 1971, 58, 372-395.
47
48 [31] Chimote, A. A., Adragna, N. C., Lauf, P. K., *J. Cell. Physiol.* 2010, 223, 110-122.
49
50 [32] Kasner, S. E., Ganz, M. B., *Am. J. Physiol.* 1992, 262, F462-F467.
51
52
53
54
55
56
57
58
59
60

- 1
2
3 [33] Andersson, B., Janson, V., Behnam-Motlagh, P., Henriksson, R., Grankvist, K.,
4
5 *Toxicol. In Vitro* 2006, *20*, 986-994.
6
7 [34] Dallaporta, B., Hirsch, T., Susin, S. A., Zamzami, N., Larochette, N., Brenner, C.,
8
9 Marzo, I., Kroemer, G., *J. Immunol.* 1998, *160*, 5605-5615.
10
11 [35] Vermes, I., Haanen, C., Steffens-Nakken, H., Reutelingsperger, C., *J. Immunol.*
12
13 *Meth.* 1995, *184*, 39-51.
14
15 [36] Schneider, C. A., Rasband, W. S., Eliceiri, K. W., *Nat. Methods* 2012, *9*, 671-675.
16
17 [37] Copp, J., Wiley, S., Ward, M. W., van der Geer, P., *Cell Physiol.* 2005, *288*,
18
19 C403-C415.
20
21 [38] Rouzai-Dubois, B., Ouanounou, G., O'Regan, S., Dubois, J. M., *Eur. J. Physiol.*
22
23 2009, *457*, 1187-1198.
24
25 [39] Hamann, S., Herrera-Perez, J. J., Zeuthen, T., Alvarez-Leefmans, F. J., *J. Physiol.*
26
27 2010, *588*, 4089-4101.
28
29 [40] Katkov, I. I., *Cryobiology* 2011, *62*, 232-241.
30
31 [41] Dezaki, K., Maeno, E., Sato, K., Akita, T., Okada, Y., *Apoptosis* 2012, *17*, 821-
32
33 831.
34
35
36
37
38
39

Figure Legends:

40
41 **Figure 1.** Modelled frequency dependence of the Clausius-Mossotti (CM) factor for
42 mouse lymphocytes suspended in medium conductivities of 50, 200 and 300 mS/m,
43 based on the dielectric data of Asami *et al* [26]. The DEP cross-over frequency f_{x01}
44 varies with the medium conductivity, whereas f_{x02} remains constant.
45
46
47
48
49
50

51
52 **Figure 2.** Forward (FSC) and side-scatter (SSC) plots (25,000 event counts) obtained
53 concurrently with DEP experiments for cells suspended in the (a) culture medium; (b)
54
55
56
57

1
2
3 270 mOsm medium; (c) 310 mOsm medium; (d) 350 mOsm medium. A clear trend is
4 evident of a reduction in FSC and increase in SSC with increasing osmolarity. The
5 number at the top-right of each plot gives the percentage of intact cells, as determined
6 by changes in the overall FSC and SSC heights.
7
8
9

10
11
12
13 **Figure 3.** Plots of forward scatter height (FSC-H) versus propidium iodide uptake
14 (FL2-H) by the cells. Each plot represents 25,000 cells in either (a) the culture
15 medium, or DEP medium of osmolarity (b) 270 mOsm; (c) 310 mOsm; (d) 350
16 mOsm. The numbers given in the gated regions give an estimate of the proportion of
17 cells with intact and impermeant membranes. Bands of signals from apoptotic bodies
18 and cell fragments appear below the gated regions.
19
20
21
22
23
24
25
26
27
28

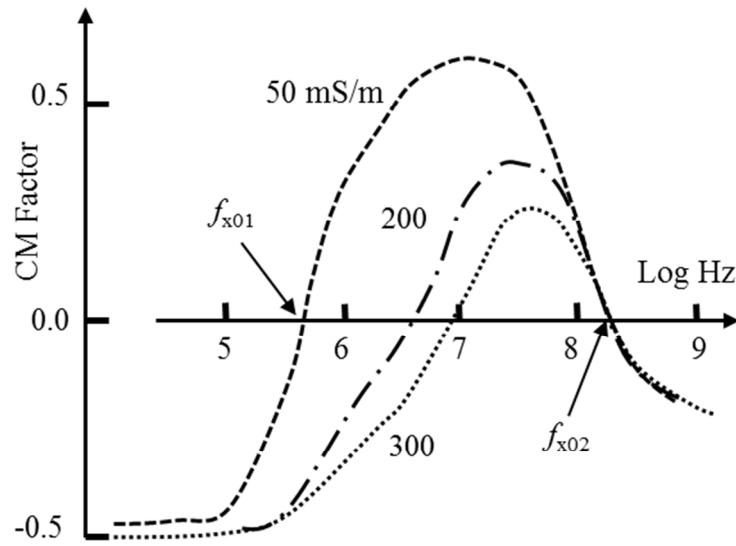
29 **Figure 4.** Boyle-van't Hoff plot for the murine myeloma cells, with the mean \pm 95%
30 confidence intervals shown (based on a spherical shape). The inset figure shows the
31 variation of cell volume with osmolarity, where the isotonic volume was determined
32 for cells suspended in PBS.
33
34
35
36
37
38
39

40 **Figure 5.** • Values of the cross-over frequency f_{x01} decrease with increasing
41 osmolarity of the suspending medium, whereas f_{x02} (o data points) exhibits the
42 opposite trend. The deviation above 215 mOsm of the experimental data points (o)
43 for f_{x02} from that predicted by Equation (6) is discussed in the main text. All data
44 points were obtained for a medium conductivity 41.5 mS/m. Error bars give \pm 95%
45 confidence levels.
46
47
48
49
50
51
52
53
54
55
56
57
58
59
60

1
2
3 **Figure 6.** Flow cytometry analysis of PBFI fluorescence ratio, as a percentage of that
4 obtained for the PBFI loaded control cells, in phosphate buffered saline solutions at
5 different osmolarities. Error bars give $\pm 95\%$ confidence levels.
6
7
8
9

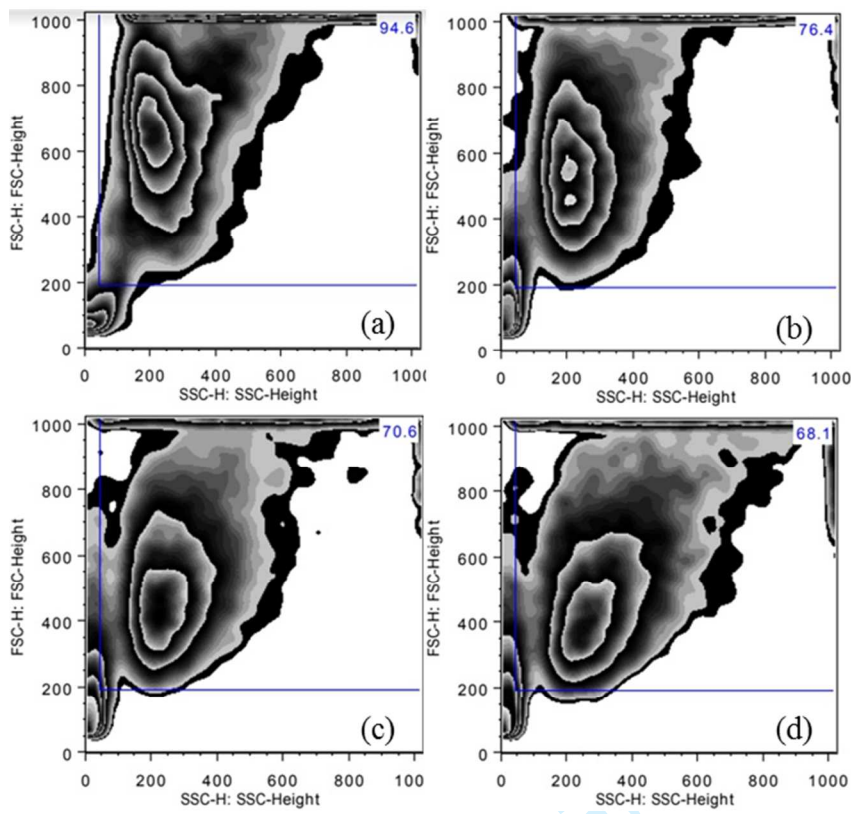
10
11 **Figure 7.** A linear relationship exists between values of the cross-over frequency f_{x02}
12 and the PBFI fluorescence ratio determined from flow cytometry measurements.
13 Error bars give $\pm 95\%$ confidence levels.
14
15
16
17
18

19
20 **Figure 8.** Dependence of membrane capacitance C_m with medium osmolarity,
21 determined using Equation (1) from measurements of f_{x01} and the mean cell diameter
22 of 50 cells suspended at each osmolarity value for a medium conductivity of 41.5
23 mS/m. A negligibly small value was assumed for the membrane conductance G_m .
24
25
26
27
28
29
30
31
32
33
34
35
36
37
38
39
40
41
42
43
44
45
46
47
48
49
50
51
52
53
54
55
56
57
58
59
60

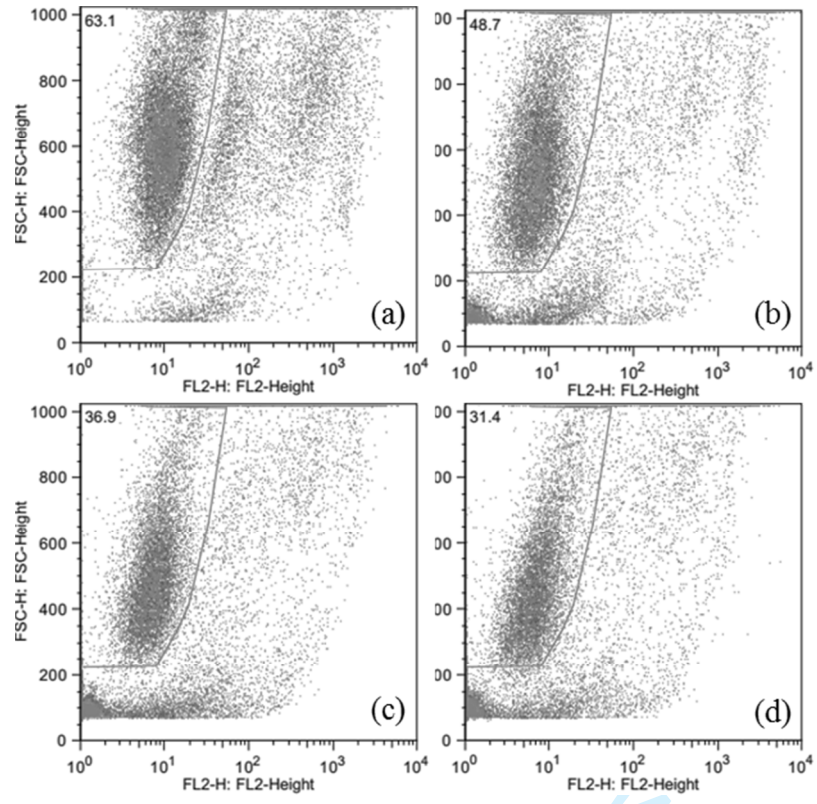


review

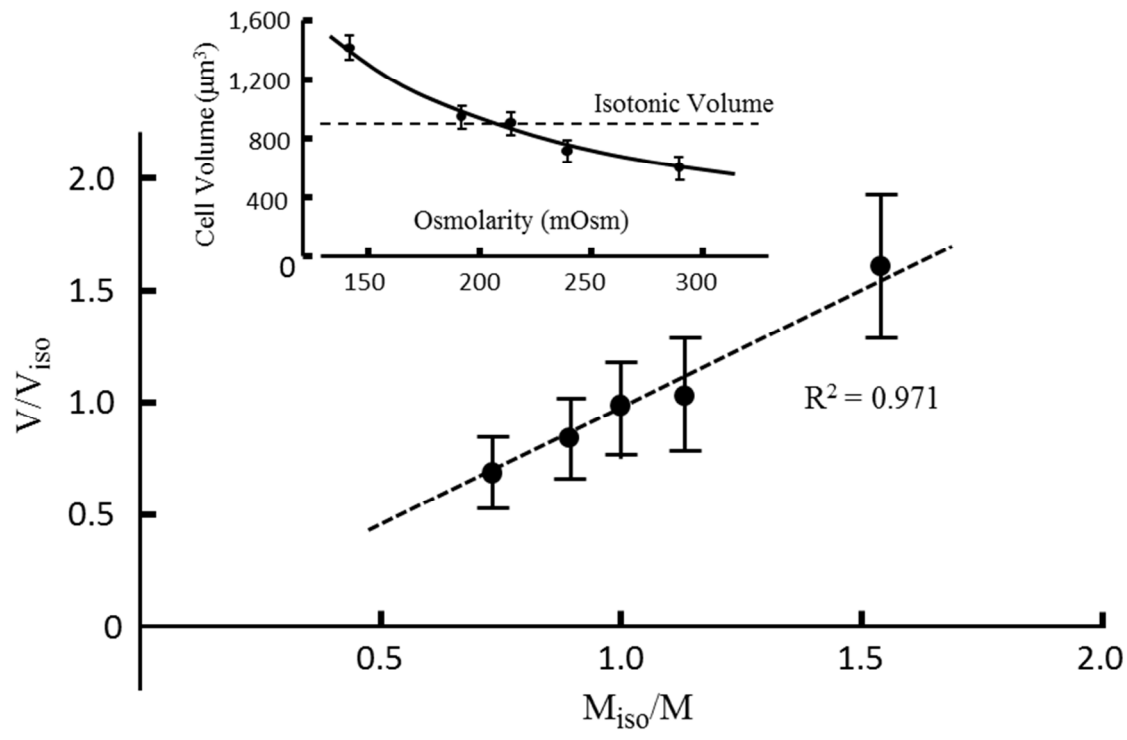
1
2
3
4
5
6
7
8
9
10
11
12
13
14
15
16
17
18
19
20
21
22
23
24
25
26
27
28
29
30
31
32
33
34
35
36
37
38
39
40
41
42
43
44
45
46
47
48
49
50
51
52
53
54
55
56
57
58
59
60

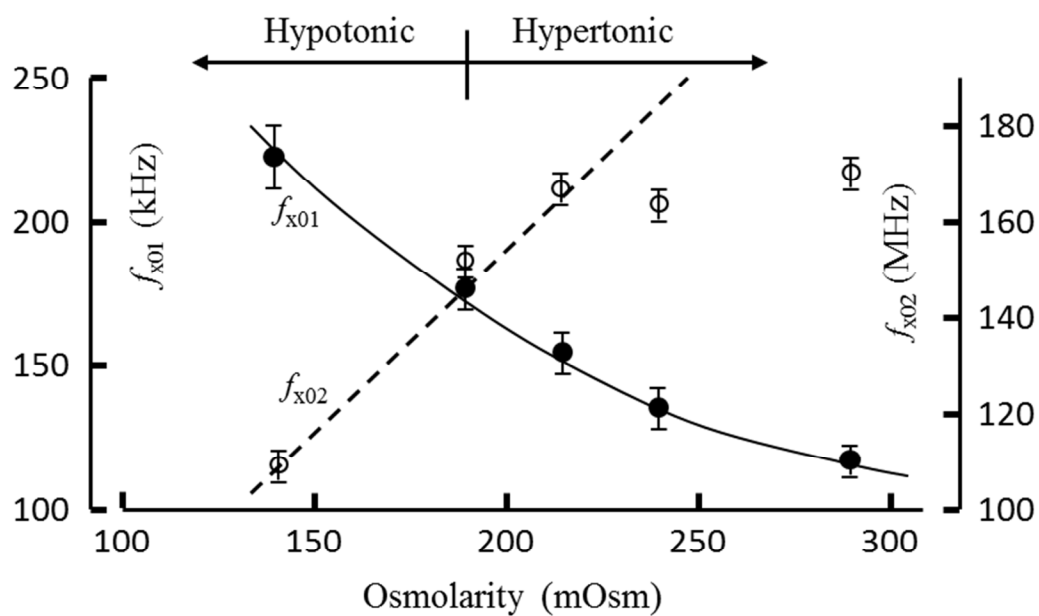


1
2
3
4
5
6
7
8
9
10
11
12
13
14
15
16
17
18
19
20
21
22
23
24
25
26
27
28
29
30
31
32
33
34
35
36
37
38
39
40
41
42
43
44
45
46
47
48
49
50
51
52
53
54
55
56
57
58
59
60

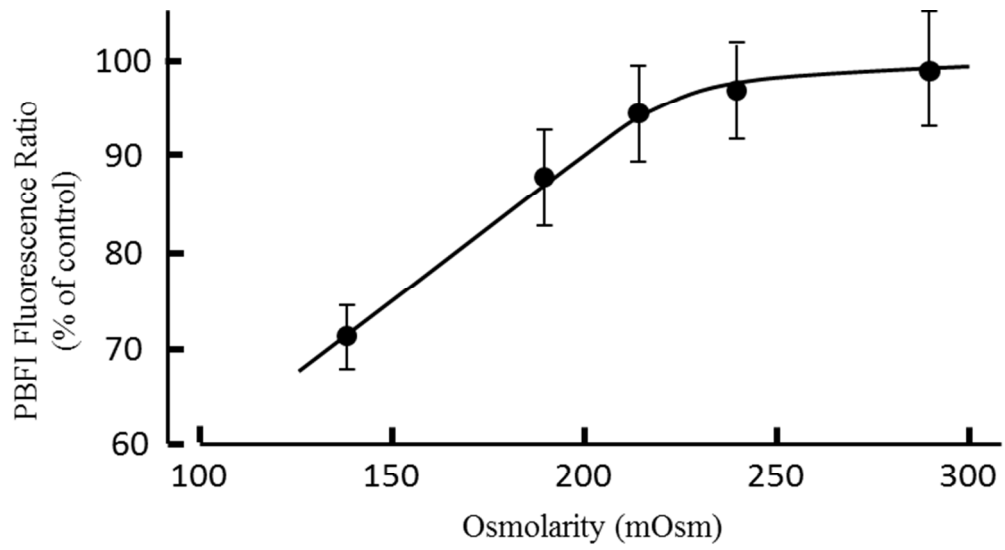


1
2
3
4
5
6
7
8
9
10
11
12
13
14
15
16
17
18
19
20
21
22
23
24
25
26
27
28
29
30
31
32
33
34
35
36
37
38
39
40
41
42
43
44
45
46
47
48
49
50
51
52
53
54
55
56
57
58
59
60

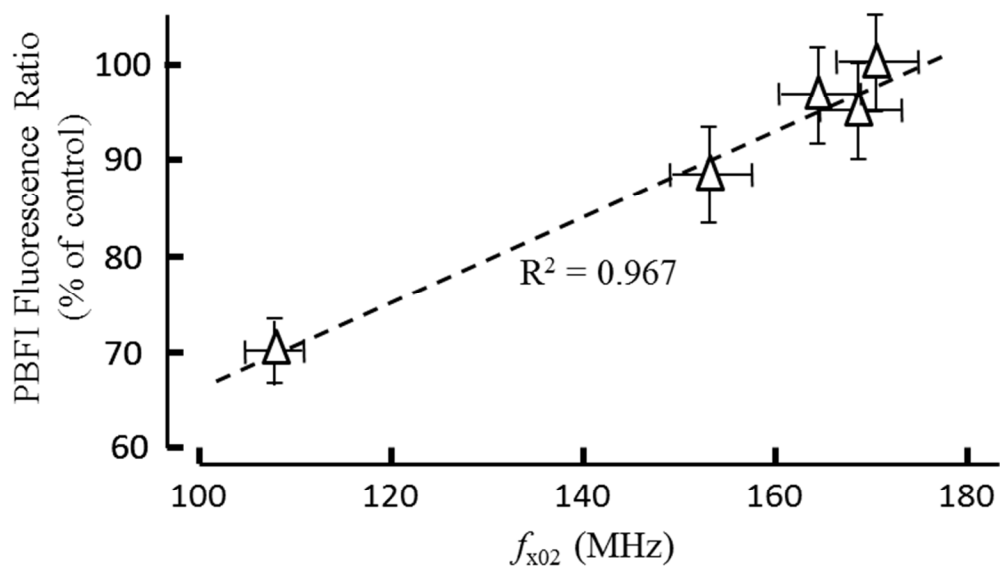




1
2
3
4
5
6
7
8
9
10
11
12
13
14
15
16
17
18
19
20
21
22
23
24
25
26
27
28
29
30
31
32
33
34
35
36
37
38
39
40
41
42
43
44
45
46
47
48
49
50
51
52
53
54
55
56
57
58
59
60

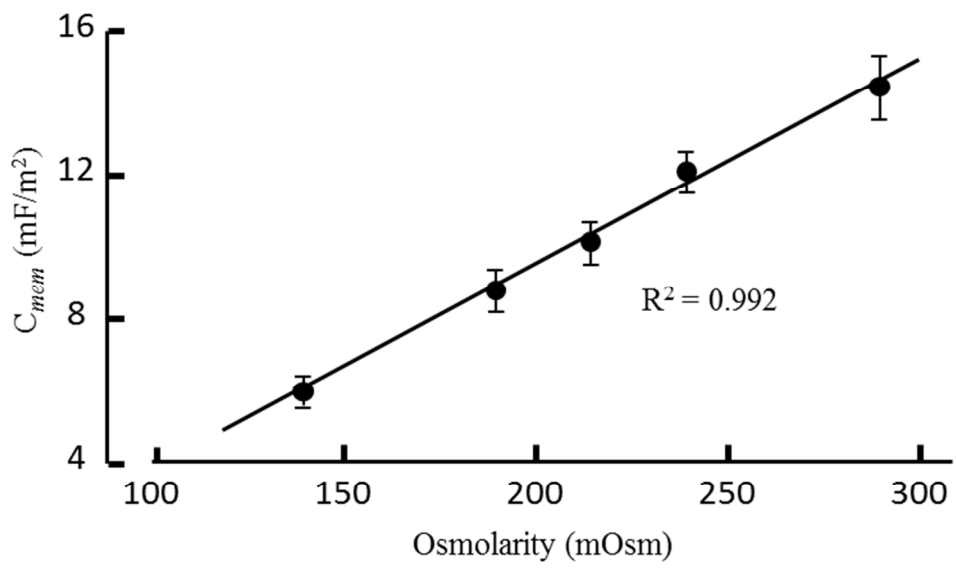


review



review

1
2
3
4
5
6
7
8
9
10
11
12
13
14
15
16
17
18
19
20
21
22
23
24
25
26
27
28
29
30
31
32
33
34
35
36
37
38
39
40
41
42
43
44
45
46
47
48
49
50
51
52
53
54
55
56
57
58
59
60



Review